

Factors Controlling Photochemical Cleavage of the Energetically Unfavorable Ph–Se Bond of Alkyl Phenyl Selenides

Akihiko Ouchi,^{*,†,‡} Suyou Liu,^{†,§} Zhong Li,^{†,§} S. Ajaya Kumar,^{†,§} Toshiaki Suzuki,[†] Takeshi Hyugano,[‡] and Haruo Kitahara[¶]

National Institute of Advanced Industrial Science and Technology (AIST), Tsukuba, Ibaraki 305-8565, Japan, the University of Tsukuba, Ibaraki 305-8571, Japan, and Faculty of Education, Hirosaki University, Hirosaki 036-8560, Japan

ouchi.akihiko@aist.go.jp

Received July 4, 2007



Primary photochemical paths of alkyl phenyl selenides (**1**) were investigated, and an origin of large deviations in the chemical yields of products obtained by carbon radical reactions induced by photolysis of phenyl selenides was clarified. KrF excimer laser photolyses of *n*-pentyl phenyl selenide (**1a**) yielded 1-pentene (**2a**), *n*-pentane (**3a**), *n*-decane (**4a**), dipentyl selenide (**5a**), benzene (**6**), dipentyl diselenide (**7a**), and diphenyl diselenide (**7**) as major photoproducts, with compounds **2a**, **3a**, **4a**, **5a**, and **7** formed by pentyl–Se bond cleavage, and **5a**, **6**, and **7a** by Ph–Se bond cleavage. The selectivity of the photoproducts revealed the occurrence of an unexpected amount of Ph–Se bond cleavage (35% in *n*-hexane at 248 nm) during photolysis. Solvent viscosity, wavelength of light, and the structure of alkyl substituents were the major factors that controlled Ph–Se bond cleavage. The ratio of Ph–Se bond cleavage decreased with increasing solvent viscosity and laser wavelength. The effect of alkyl substituents on the ratio of bond cleavages, Ph–Se/total C–Se, was investigated for five alkyl phenyl selenides; the ratio decreased in the order pentyl > 2-methylallyl > allyl > 1-ethylpropyl > *tert*-butyl groups. The contribution of Ph–Se bond cleavage is most probably the origin of the large deviations in the yields of radical reactions induced by photolyses of **1**, which can be minimized by selecting appropriate solvents and wavelength of light.

Introduction

The phenylselenenyl group is a useful functional group that is often used in organic synthesis. One of the applications of the phenylselenenyl group is C–C bond formation through radical reactions, in which carbon radicals are generated by PhSe–C bond cleavage.¹ It is generally believed that alkyl phenyl

selenides undergo preferential cleavage of alkyl–Se rather than Ph–Se bonds by photolysis because C–Se bond dissociation energy is greater for Ph–Se than for alkyl–Se bonds.² On the basis of this belief, a number of reactions using photochemical PhSe–alkyl bond cleavage have been reported for various alkyl phenyl selenides,³ but the photochemical selectivity of Ph–Se and alkyl–Se bond cleavage has not been investigated systematically. Indeed, large deviations in the yields of expected products are often observed in these reactions, for which the reason has not been clarified so far.

[†] AIST.

[‡] University of Tsukuba.

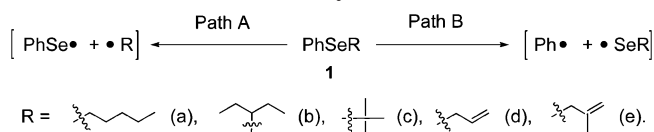
[¶] Hirosaki University.

[§] Present affiliations: Central South University, P. R. China (S.L.), East China University of Science and Technology, P. R. China (Z.L.), St. Mary's College, India (S.A.K.), and RIKEN Wako Institute, Japan (T.S.).

(1) (a) Martens, J.; Praekcke, K. *J. Organomet. Chem.* **1980**, *198*, 321–351. (b) Goldschmidt, Z. In *The Chemistry of Organic Selenium and Tellurium Compounds*; Patai, S., Ed.; John Wiley & Sons: Chichester, 1987; Vol. 2, Chapter 5. (c) Schiesser, C. H.; Wild, L. M. *Tetrahedron* **1996**, *52*, 13265–13314. (d) Renaud, P. *Top. Curr. Chem.* **2000**, *208*, 81–112.

(2) Dissociation energies of C–Se bonds are 59.9 kcal·mol^{−1} for Et₂Se and 71 kcal·mol^{−1} for Ph₂Se: Batt, L. In *The Chemistry of Organic Selenium and Tellurium Compounds*; Patai, S., Rappoport, Z., Eds.; John Wiley & Sons: Chichester, 1986; Vol. 1, p 159.

SCHEME 1. The Two Primary Photochemical Paths of 1



To understand the origin of the large deviations in the yields and to improve the synthetic efficiency of the reactions, it is necessary to understand the photochemical reactivity of the selenides. Therefore, we conducted a detailed study of the photolysis of simple alkyl phenyl selenides: *n*-pentyl (**1a**), 1-ethylpropyl (**1b**), *tert*-butyl (**1c**), allyl (**1d**), and 2-methylallyl (**1e**) phenyl selenides (Scheme 1). To the best of our knowledge, systematic studies on the photochemical reactivity of C–Se bond cleavage of selenides have not been conducted. In the present study, we found a significant amount of Se–Ph bond cleavage (Path B in Scheme 1) in addition to the normal alkyl–SePh bond cleavage (Path A in Scheme 1), the ratio of which was dependent on the wavelength of light, solvent viscosity, and the structure of alkyl groups. On the basis of these results, the synthetic efficiency of the reactions of organoselenium compounds can be increased by selecting suitable reaction conditions revealed in the present study.

Results and Discussion

Absorption Spectra of 1a–e. Figure 1 shows the absorption spectra of **1a–e**. The figure shows the presence of four absorption bands for each compound, which are attributed to the PhSe moiety of the molecules. The photolyses were conducted with ArF (193 nm), KrF (248 nm), and XeCl (308 nm) excimer lasers, with emissions corresponding to the different absorption bands of **1**. The absorption at 308 nm corresponds to a secondary absorption band of a phenyl ring (π – π^* , $^1\text{L}_b$),⁴ that at 248 nm to π – π^* ($^1\text{L}_b$)⁴ absorption and to an *n*– π^* transition of the Se atom,⁵ and that at 193 nm to higher π – π^* transitions.

KrF Excimer Laser Photolysis of 1a. First, photolysis of **1a** was conducted with a KrF excimer laser. Scheme 2 shows the major photoproducts of **1a** in *n*-hexane at room temperature.

The product distribution during KrF excimer laser photolysis is shown in Figure 2. With the decrease in **1a**, photoproducts **2a–5a**, **6**, **7**, and **7a** were formed with different selectivity.⁶ A significant increase in the selectivity of **6** and a decrease in **7** were observed as photolysis progressed, in contrast to small

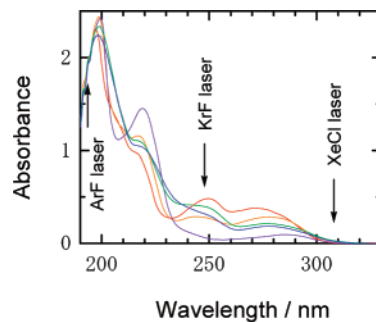


FIGURE 1. Absorption spectra of **1a–e**. **1a** (red); **1b** (orange); **1c** (purple); **1d** (green); **1e** (blue). Concentration: 10^{-4} M in *n*-hexane, optical path: 10 mm. The wavelengths of the ArF, KrF, and XeCl excimer laser emissions are marked in the figure.

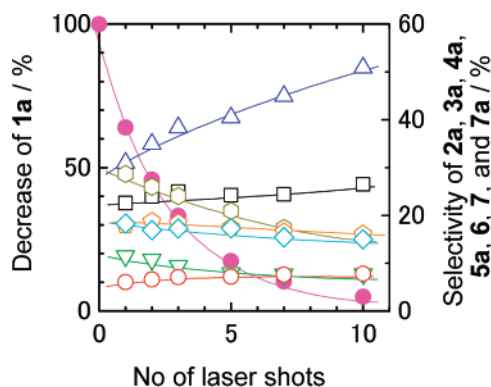


FIGURE 2. KrF excimer laser photolysis of **1a**. Decrease in **1a** (magenta ●) and selectivity⁶ of 1-pentene (**2a**, black □), *n*-pentane (**3a**, red ○), *n*-decane (**4a**, green ▽), dipentyl selenide (**5a**, turquoise ◇), benzene (**6**, blue △), diphenyl diselenide (**7**, brown ○), and dipentyl diselenide (**7a**, orange ○) as a function of the number of the laser shots.¹⁴ Concentration: 10^{-3} M in *n*-hexane, optical path: 1 mm, laser fluence: $100 \text{ mJ cm}^{-2} \text{ pulse}^{-1}$, room temperature.

changes in the selectivity of **2a–5a** and **7a**. The considerable changes in **6** and **7** indicate the presence of a secondary photolysis of **7** to form **6**, which was confirmed by a KrF laser photolysis of **7** in *n*-hexane.⁷

Figure 2 also shows a slight increase in the selectivity of **2a** and **3a**, with a small decrease in the selectivity of **5a** as photolysis progressed. The small change in selectivity of **2a**, **3a**, and **5a** can be explained by the generation of **2a** and **3a** via secondary photolysis of **5a**, which was confirmed by a KrF laser photolysis of **5a** in *n*-hexane.⁷

Primary Products of KrF Excimer Laser Photolysis of 1a. The formation of **2a**, **3a**, and **4a** can be explained by the reactions of pentyl radicals that were formed by the expected primary photochemical cleavage of pentyl–Se bonds. However, a considerable amount of benzene (**6**) was also surprisingly formed, even after a single laser shot. This result indicates that **6** was also formed by a primary photochemical process via an unexpected photochemical Ph–Se bond cleavage to generate phenyl radicals and subsequent hydrogen abstractions because the occurrence of secondary photolysis is unlikely within the pulse duration of the KrF laser (23 ns, fwhm). Furthermore, the possibility of the formation of phenyl radicals by thermal decomposition of photochemically generated PhSe radicals can be also excluded because PhSe radicals are reported to undergo

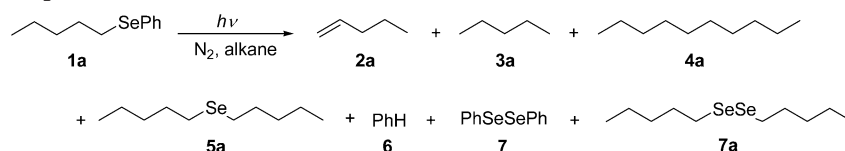
(3) (a) Byers, J. H.; Lane, G. C. *J. Org. Chem.* **1993**, *58*, 3355–3360. (b) Renaud, P.; Vionnet, J.-P. *J. Org. Chem.* **1993**, *58*, 5895–5896. (c) Curran, D. P.; Eichenberger, E.; Collis, M.; Roepel, M. G.; Thoma, G. *J. Am. Chem. Soc.* **1994**, *116*, 4279–4288. (d) Ryu, I.; Muraoka, H.; Kambe, N.; Komatsu, M.; Sonoda, N. *J. Org. Chem.* **1996**, *61*, 6396–6403. (e) Back, T. G.; Gladstone, P. L.; Parrez, M. *J. Org. Chem.* **1996**, *61*, 3806–3814. (f) Wackernagel, F.; Schwiter, U.; Giese, B. *Tetrahedron Lett.* **1997**, *38*, 2657–2660. (g) Ouchi, A.; Koga, Y. *J. Org. Chem.* **1997**, *62*, 7376–7383. (h) Buers, J. H.; Shaughnessy, E. A.; Mackie, T. *Heterocycles* **1998**, *48*, 2071–2077. (i) Ouchi, A.; Sakuragi, M.; Kitahara, H.; Zandomeneghi, M. *J. Org. Chem.* **2000**, *65*, 2350–2357. (j) Ouchi, A.; Li, Z.; Sakuragi, M.; Majima, T. *J. Am. Chem. Soc.* **2003**, *125*, 1104–1108. (k) Murakami, S.; Kim, S.; Ishii, H.; Fuchigami, T. *Synlett* **2004**, 815–818. (l) Murakami, S.; Ishii, H.; Fuchigami, T. *J. Fluorine Chem.* **2004**, *125*, 609–614. (m) Hong, I. S.; Greenberg, M. M. *Org. Lett.* **2004**, *6*, 5011–5013. (n) Pandey, G.; Gadre, S. R. *Acc. Chem. Res.* **2004**, *37*, 201–210.

(4) Jaffé, H. H.; Orchin, M. *Theory and Application of Ultraviolet Spectroscopy*; John Wiley & Sons: New York, 1962; Chapter 12, Section 12.2.

(5) Mason, W. R. *J. Phys. Chem.* **1996**, *100*, 8139–8143.

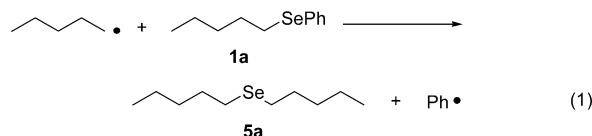
(6) Product selectivity is based on the consumption of **1**.

(7) Original data are provided as Supporting Information.

SCHEME 2. Major Photoproducts of **1a**

predominant recombination to **7**.⁸ The formation of **5a**, which is a coupling product of pentyl and pentylselenyl radicals, also supports the presence of primary Ph–Se bond cleavage.

Another possible primary process for the formation of **6** is a reaction between photochemically generated pentyl radicals and **1a** to form **5a** and phenyl radicals (eq 1) and successive hydrogen abstraction by the phenyl radicals. However, this reaction path can be excluded from the major process because **7a**, which cannot be formed by the process shown in eq 1, was observed in the photolysis. In addition, Figure 2 shows that the selectivity of diphenyl diselenide (**7**) and dipentyl diselenide (**7a**) is 29 and 17%, respectively, and if we assume that the efficiency for the formation of diselenides is the same between **7** and **7a**, the ratio $29/17 = 1.7$ is similar to the ratio of pentyl–Se and Ph–Se bond cleavage, $58/31 = 1.9$ (see Table 1).



The total selectivity of the major photoproducts from pentyl and phenyl radicals generated by primary photochemical processes, that is, the sum of the selectivity for **2a**, **3a**, **4a**, **5a**, and **6** after one laser shot, was 89.3%, which indicates that most of the primary photochemical processes can be explained by analyses of the major products. However, the total selectivity increases to 97.1% when the selectivity of minor products is included, that is, pentylbenzene, undecane, and 2- and 4-pentylphenyl phenyl diselenides.⁷

Formation of Benzene (6) in KrF Excimer Laser Photolysis of 1a. Details on the formation of **6** were further investigated by experiments on the effect of laser intensity. Figure 3 shows the consumption of **1a** and the yields of **2a–4a** and **6** as a function of KrF laser fluence in a double-logarithmic plot. The experiments were conducted with a single laser pulse to avoid secondary photochemical processes. It is evident that the slope for consumption of **1a** and for yields of **2a**, **3a**, and **6** is unity, whereas that for the yield of **4a** is 2. These results indicate that the consumption of **1a** and the formation of **2a**, **3a**, and **6** proceeded by one-photon processes, while the formation of **4a** is by a two-photon process. The fact that **6** was formed by a one-photon process is clear evidence that **6** is a primary photoproduct formed by initial Ph–Se bond cleavage and successive hydrogen abstraction by the phenyl radicals thus generated.

The hydrogen source for the formation of **6** from phenyl radicals was investigated by KrF laser photolysis of *n*-C₅D₁₁-SePh (**1a-d₁₁**) in *n*-hexane. GC–MS analysis of photochemically generated **6** showed that 92% was C₆H₆ (**6**) and 8% was C₆H₅D (**6-d₁**). This result indicates that 92% of the hydrogen was abstracted from the solvent. To clarify the source of the deuterium in **6-d₁**, experiments on the effect of laser intensity

were conducted with **1a-d₁₁**, for which the results are shown in Figure 4. The slope for the yield of **6** is unity, but that for **6-d₁** is 1.6. The result for **6-d₁** indicates that 40% of **6-d₁** was formed by one-photon processes and 60% by a two-photon process. The deuterium atom of the one-photon processes is most probably abstracted from pentyl-*d₁₁*-selenyl radicals, both inside and outside of the solvent cages, and that of the two-photon process from pentyl-*d₁₁* radicals. Possible deuterium abstraction from the starting material **1a-d₁₁** can be neglected because such radicals generated from **1a-d₁₁** would yield products that are different from the primary products, while the mass balance of the primary products was found to be 97.1% (vide supra).

From the selectivity of **6** of 30.9%, it was calculated that hydrogen abstraction by phenyl radicals proceeded at levels of 28.4% from the solvent, 1.0% from pentylselenyl radicals, and 1.5% from pentyl radicals. The two-photon process observed in this experiment is contradictory to the laser intensity results

TABLE 1. Selectivity of C–Se Bond Cleavages of **1a**

light source ^a	selectivity of C–Se bond cleavage (%) ^b			ratio ^f (Ph–Se/total)
	pentyl–Se ^c	Ph–Se ^d	total ^e	
ArF laser (193 nm)	38.5	25.0	63.5	0.39
KrF laser (248 nm)	58.4	30.9	89.3	0.35
XeCl laser (308 nm)	68.4	27.6	96.0	0.29

^a Laser photolysis conditions: 10^{−3} M **1a** in *n*-hexane, optical path: 1 mm, room temperature; laser intensity: 1.25 × 10¹⁷ photons cm^{−2} pulse^{−1}, number of laser shots: 1 shot (ArF and KrF) and 100 shots (XeCl). Original data are provided as Supporting Information. ^b Product selectivity is based on the consumption of **1**, and results are the average of at least two independent runs. ^c Selectivity of (**2a** + **3a** + **4a** + **5a**). ^d Selectivity of **6**. ^e Selectivity of (**2a** + **3a** + **4a** + **5a** + **6**). ^f Selectivity ratio of **6**/(**2a** + **3a** + **4a** + **5a** + **6**).

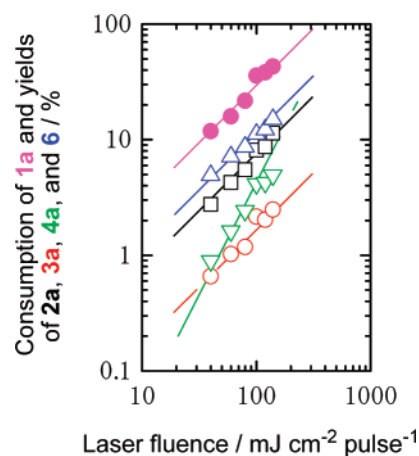
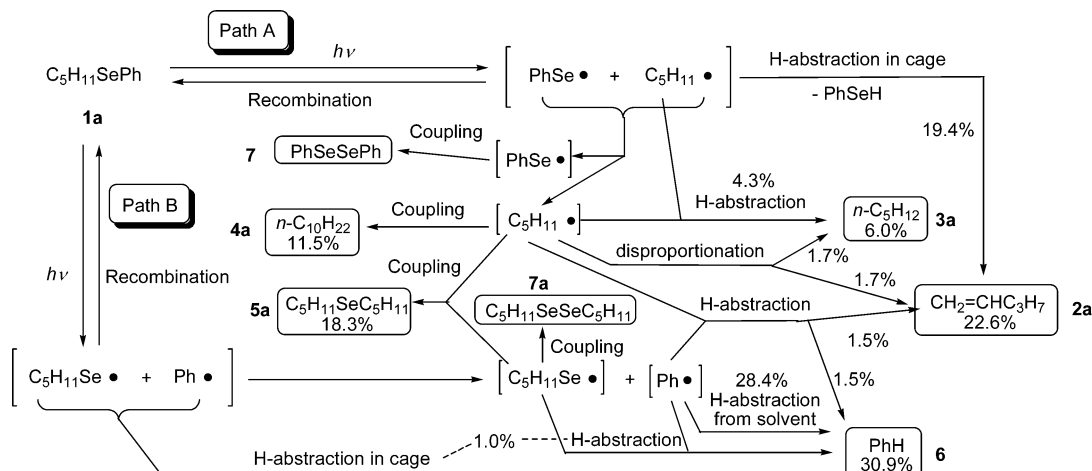


FIGURE 3. Fluence dependence on the KrF excimer laser photolysis of **1a**. Consumption of **1a** (magenta ●) and yields of 1-pentene (**2a**, black □), *n*-pentane (**3a**, red ○), *n*-decane (**4a**, green ▽), and benzene (**6**, blue △) as a function of the laser fluence.¹⁴ Concentration: 10^{−3} M in *n*-hexane, number of laser shots: 1 shot, optical path: 1 mm, room temperature.

(8) Ito, O. *J. Am. Chem. Soc.* **1983**, *105*, 850–853.

SCHEME 3. Plausible Reaction Mechanism for the Formation of Major Photoproducts of **1a** (The Selectivity⁶ of the Primary Products and Reaction Paths Are Also Indicated)



for the formation of **6** from **1a** (cf. Figure 3), but this can be rationalized on the basis of a small contribution of the two-photon process in the formation of **6** compared to the one-photon processes.

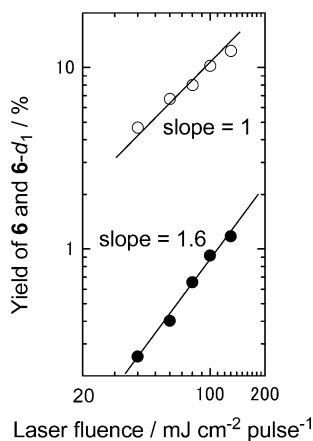


FIGURE 4. Laser fluence effect on the yield of benzene (**6**, ○) and benzene-*d*₁ (**6-d**₁, ●) in KrF excimer laser photolysis of **1a-d**₁₁ as a function of the laser fluence.¹⁴ Concentration: 10⁻³ M in *n*-hexane, number of laser shots: 1 shot, optical path: 1 mm, room temperature.

Reaction Mechanism of KrF Excimer Laser Photolysis of **1a.** Scheme 3 shows a plausible reaction mechanism for the formation of primary photoproducts of **1a**, with selectivity⁶ of the major products also presented. Although the mass balance of photoproducts was good, there are still some byproducts that were not identified. However, we think that there is only a very small contribution of secondary photolysis in these unidentified products because the occurrence of secondary photolyses is less probable particularly at one laser shot (within ca. 20 ns).

The requirement for two photons for the formation of **4a** is consistent with the reaction mechanism shown in Scheme 3. Considering that the selectivity of **4a** for one laser shot was 11.5% and the disproportionation/coupling ratio of primary alkyl radicals is 0.15,⁹ it was calculated that 1.7% of **2a** and **3a** was formed by disproportionation. The selectivity of **3a** for one laser shot was 6.0%, so that 4.3% of **3a** should be formed by

hydrogen abstractions from the solvent. This was confirmed by the photolysis of **1a-d**₁₁ in *n*-hexane; GC–MS analysis of photochemically generated **3a** showed a major peak at *m/e* 83 corresponding to C₃HD₁₁, which provides evidence of hydrogen abstraction from the solvent.

The selectivity of **2a** for one laser shot was 22.6% and as 1.7% was formed by disproportionation and 1.5% by hydrogen abstraction by phenyl radicals, 19.4% of **2a** was formed by other processes. Other possible paths for the formation of **2a** are (i) an intramolecular β-H elimination¹⁰ in **1a**, (ii) hydrogen abstractions from pentyl radicals by PhSe or pentylselenyl radicals on the outside of the solvent cage, and (iii) hydrogen abstraction of pentyl radicals by PhSe radicals within the solvent cage.

To determine the path responsible for the formation of **2a** from the three possible paths, experiments on the effect of solvent viscosity were conducted. A series of experiments was conducted in *n*-heptane, *n*-dodecane, *n*-tetradecane, *n*-hexadecane, cyclopentane, cyclohexane, cycloheptane, cyclooctane, and cyclododecane.⁷ Figure 5 shows the selectivity of **2a**, **3a**, **4a**, **5a**, and **6** and the consumption of **1a** for a single KrF laser shot as a function of solvent viscosity.¹¹

Figure 5a clearly shows that the selectivity of **2a** increased with increasing solvent viscosity. If the formation of **2a** proceeded by path (i), an intramolecular β-H elimination, **2a** and PhSeH would be formed within the solvent cage, so the solvent viscosity should not have much effect on the selectivity of **2a**; however, this was not the case, as shown in Figure 5a.

It has been reported that the fraction of geminate radical pairs escaping from the solvent cage is a linear function of (1/η)^{*n*}, where η is the solvent viscosity and the value of *n* is between 0.5¹² and 1.0.¹³ This means that the selectivity of products formed from free radical species outside the solvent cage will

(10) (a) Pickett, N. L.; Foster, D. F.; Maung, N.; Cole-Hamilton, D. J. *J. Mater. Chem.* **1999**, *9*, 3005–3014. (b) Pola, J.; Ouchi, A. *J. Organomet. Chem.* **2001**, *629*, 93–96.

(11) Riddick, J. A.; Toops, E. E., Jr. *Technique of Organic Chemistry*, 2nd ed.; Interscience Publishers: New York, 1955; Vol. VII, Chapter III.

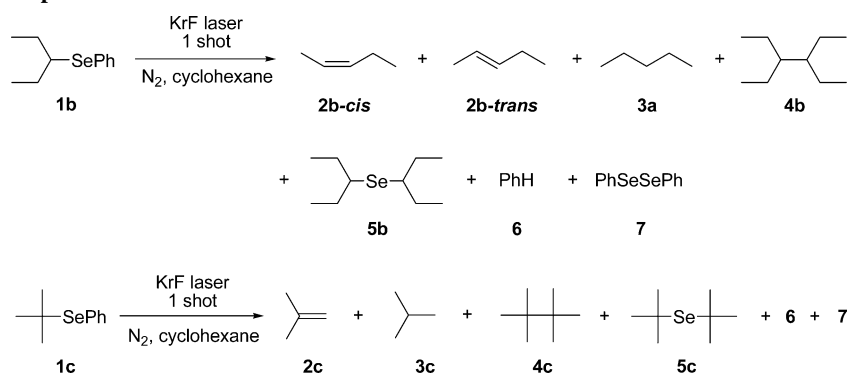
(12) Koenig, T.; Deinzer, M. *J. Am. Chem. Soc.* **1968**, *90*, 7014–7019.

(13) Niki, E.; Kamiya, Y. *J. Am. Chem. Soc.* **1974**, *96*, 2129–2133.

(14) Results are the average of at least two independent runs.

(15) In the case of tetradecane, the selectivity of **5a** was not determined owing to the overlapping of the peaks for tetradecane and **5a** in GLC analyses.

(9) Fossey, J.; Lefort, D.; Sorba, J. *Free Radicals in Organic Chemistry*; John Wiley & Sons: Chichester, 1995; p 124, Table 10.3.

SCHEME 4. Major Photoproducts of **1b** and **1c**

decrease with increasing solvent viscosity. Indeed, the selectivity of products formed solely on the outside of the solvent cage (i.e., **4a** and **5a**) decreased with increasing solvent viscosity. However, the trend for selectivity of **2a** was opposite to the case expected from path (ii).

The trend observed for selectivity of **2a** is consistent with the result expected from path (iii). The contribution of hydrogen abstraction from pentyl radicals by PhSe radicals within the solvent cage to form **2a** will increase when the radical pair is retained within the cage for a longer time. The decrease in consumption of **1a** with increasing solvent viscosity indicates an increase in the recombination probability for pentyl and PhSe

radicals owing to inhibition of the escape of radical pairs from the cage, which is also in accord with the trend expected from path (iii). Therefore, it is concluded that 19.4% of the formation of **2a** can be attributed to hydrogen abstraction from pentyl radicals by PhSe radicals within the solvent cage. Indeed, the formation of PhSeH was confirmed by HPLC analyses.

Solvent Viscosity Effect on the Selectivity of Pentyl–Se and Ph–Se Bond Cleavage. From the primary photochemical paths of **1a** shown in Scheme 3, we know that the ratio of pentyl–Se and Ph–Se bond cleavage (Path A vs Path B) is equal to the ratio of the selectivity (**2a** + **3a** + **4a** + **5a**) versus **6**.

Figure 6 shows the selectivity of pentyl–Se and Ph–Se bond cleavage as a function of solvent viscosity. The figure clearly shows the presence of a considerable degree of Ph–Se bond cleavage in the photolysis of **1a**, which was unexpected previously. The selectivity of Ph–Se bond cleavage increased with decreasing solvent viscosity and vice versa for the selectivity of pentyl–Se bond cleavage.

Wavelength Effect on the Selectivity of C–Se Bond Cleavage. The effect of wavelength on the selectivity of pentyl–Se and Ph–Se bond cleavage in **1a** was studied using ArF, KrF, and XeCl lasers, with results summarized in Table 1.⁷ Owing to a very low molar absorption coefficient at 308 nm (cf. Figure 1), XeCl laser photolysis was very slow so that the XeCl laser required more laser shots to achieve sufficient conversion of **1a** compared to that with the KrF and ArF lasers.

Table 1 indicates that the ratio of Ph–Se bond cleavage increased with decreasing laser wavelength. The change in the ratio probably reflects the participation of different excited states involved in photolysis because the emission wavelength of each laser corresponds to different absorption bands (cf. Figure 1).

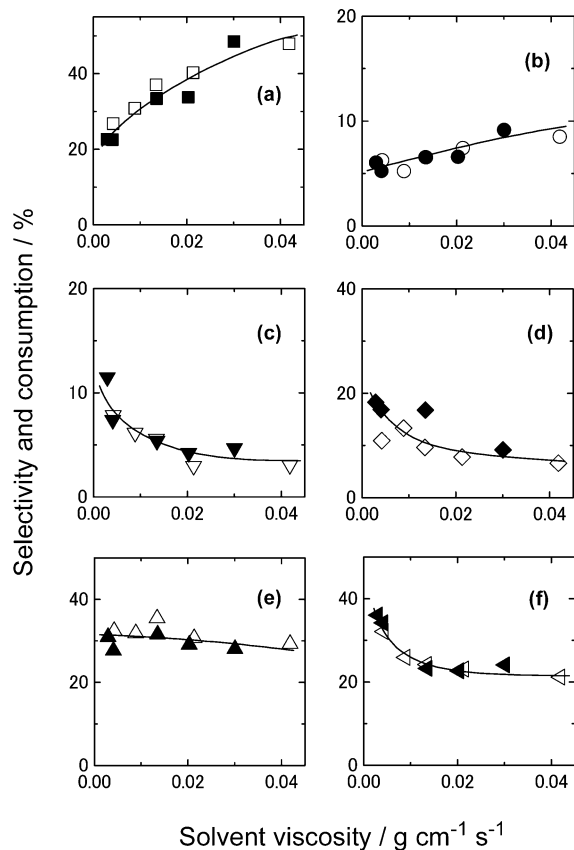


FIGURE 5. Selectivity⁶ of (a) 1-pentene (**2a**), (b) *n*-pentane (**3a**), (c) *n*-decane (**4a**), (d) dipentyl selenide (**5a**),^{11,15} (e) benzene (**6**), and (f) consumption of pentyl phenyl selenide (**1a**) in the KrF excimer laser photolysis of **1a** as a function of the solvent viscosity.^{11,14} Concentration: 10⁻³ M, optical path: 1 mm, laser fluence: 100 mJ cm⁻² pulse⁻¹, number of laser shots: 1 shot, room temperature. Open symbol: cycloalkanes; closed symbol: *n*-alkanes.

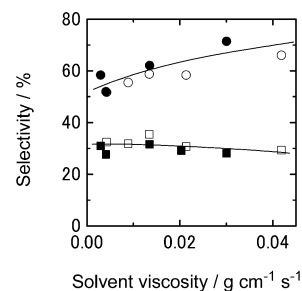
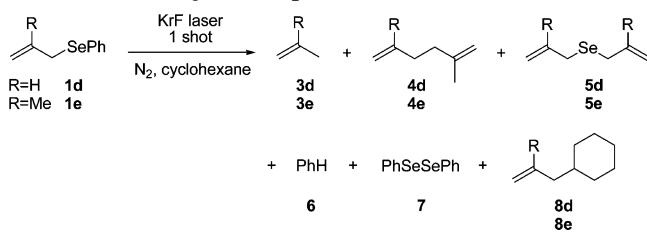


FIGURE 6. Selectivity⁶ of pentyl–Se (●, ○: **2a** + **3a** + **4a** + **5a**)¹⁵ and Ph–Se (■, □: **6**) bond cleavage in KrF excimer laser photolysis of **1a** as a function of the solvent viscosity.¹⁴ Concentration: 10⁻³ M, optical path: 1 mm, KrF excimer laser fluence: 100 mJ cm⁻² pulse⁻¹, number of laser shots: 1 shot. Open symbols: cycloalkanes; closed symbols: *n*-alkanes.

SCHEME 5. Major Photoproducts of **1d** and **1e**

The ratio of Ph–Se bond cleavage by photolysis with a low-pressure mercury lamp, which has major emission (254 nm) similar to that of the KrF laser, was 0.39 (1 min irradiation). The ratio was slightly higher than for the KrF laser, which can be explained by the formation of **6** by the previously mentioned secondary photolysis of **7**.

Effect of Alkyl Groups on the Selectivity of C–Se Bond Cleavage. The effect of alkyl substituents on the selectivity of Ph–Se and alkyl–Se bond cleavage was investigated using *n*-pentyl (**1a**), 1-ethylpropyl (**1b**), *tert*-butyl (**1c**), allyl (**1d**), and 2-methylallyl (**1e**) phenyl selenides.

The major photoproducts of **1b** and **1c** are shown in Scheme 4.⁷ In analogy with the reaction mechanism of **1a** shown in Scheme 3, the selectivity of 1-ethylpropyl–Se bond cleavage is given by the sum of the selectivity for **2b-cis**, **2b-trans**, **3a**, **4b**, and **5b** and that of the Ph–Se bond by **6**. Similarly, for **1c**, the selectivity of *tert*-butyl–Se bond cleavage is given by the sum of the selectivity for **2c**, **3c**, **4c**, and **5c** and that of the Ph–Se bond by **6**.

Scheme 5 shows the major photolysis products of **1d** and **1e**.⁷ Interestingly, a significant amount of corresponding alkylcyclohexanes (**8d**, **8e**) was detected in these cases. The selectivity of alkyl–Se bond cleavage is presented as the sum of the selectivity for **3**, **4**, **5**, and **8** and that of the Ph–Se bond by **6** for both **1d** and **1e**.

The selectivity of C–Se bond cleavage for **1a–e** is summarized in Table 2. As the alkyl substituents changed from primary to secondary and tertiary groups, the ratio of Ph–Se bond cleavage decreased, which is probably due to the decrease of alkyl–Se bond energies in this order. At the same time, the selectivity of the coupling products (**4**) decreased with increasing olefins **2**.⁷ The decrease in selectivity for **4** can be explained by the increase in the ratio of the rate constants for disproportionation/recombination as the alkyl group changes from primary (0.15) to secondary (1.2) and tertiary (4.5) groups.⁹

TABLE 2. Selectivity of C–Se Bond Cleavages of **1a–e**

substrate	selectivity of C–Se bond cleavage (%) ^a			ratio (Ph–Se/total)
	alkyl–Se	Ph–Se	total	
1a	55.5 ^b	31.8 ^c	87.3 ^d	0.36 ^e
1b	79.8 ^b	17.8 ^c	97.6 ^d	0.18 ^e
1c	92.4 ^b	2.9 ^c	95.3 ^d	0.03 ^e
1d	61.1 ^f (68.3) ^g	21.9 ^c	83.0 ^h (90.2) ⁱ	0.26 ^f (0.24) ^k
1e	48.8 ^f (56.1) ^g	22.7 ^c	71.5 ^h (78.8) ⁱ	0.32 ^f (0.29) ^k

^a Photolysis conditions: 10^{-3} M **1a–e** in cyclohexane, optical path: 1 mm, KrF laser fluence: 1.25×10^{17} photons cm^{-2} pulse⁻¹, room temperature, number of irradiated KrF laser shots: 1 shot. Product selectivity is based on the consumption of **1**, and results are the average of at least two independent runs. Original data are provided as Supporting Information. ^b Selectivity of (**2** + **3** + **4** + **5**). ^c Selectivity of **6**. ^d Selectivity of (**2** + **3** + **4** + **5** + **6**). ^e Selectivity ratio of **6**/(**2** + **3** + **4** + **5** + **6**). ^f Selectivity of (**3** + **4** + **5**). ^g Selectivity of (**3** + **4** + **5** + **8**). ^h Selectivity of (**3** + **4** + **5** + **6**). ⁱ Selectivity of (**3** + **4** + **5** + **6** + **8**). ^j Selectivity ratio of **6**/(**3** + **4** + **5** + **6**). ^k Selectivity ratio of **6**/(**3** + **4** + **5** + **6** + **8**).

For allylic groups (**1d**, **1e**), the ratio of Ph–Se bond cleavage is between that for primary and secondary alkyl groups. Disproportionation is not possible for allylic radicals, so that coupling and hydrogen abstraction are the possible radical reactions. However, owing to the stability of allylic radicals, the major reactions of allyl and 2-methylallyl radicals are coupling reactions, which is in agreement with the results for KrF laser photolyses of **1d** and **1e**.⁷ The high selectivity of alkylcyclohexanes (**8d**, **8e**), which are also coupling products of cyclohexyl radicals formed by hydrogen abstraction from solvent molecules by phenyl radicals and allylic radicals, can be also explained by the stability of allylic radicals.

Experimental Section

Synthesis of Selenides, Diselenides, and 2-Methylallylcyclohexane (8e**).** NMR spectra were recorded with CDCl_3 as solvent. As internal standards, TMS was used for ¹H NMR (δ : 0 ppm) and CDCl_3 for ¹³C NMR (δ : 77.0 ppm) analyses.

Synthesis of Alkyl Phenyl Selenides **1a–e.** Pentyl-*d*₁₁ phenyl selenide (**1a-d₁₁), 1-ethylpropyl phenyl selenide (**1b**), allyl phenyl selenide (**1d**), and 2-methylallyl phenyl selenide (**1e**) were synthesized similar to that of pentyl phenyl selenide (**1a**).¹⁶**

Pentyl Phenyl Selenide (1a**).**^{17,18} Diphenyl diselenide (3.41 g, 10.9 mmol) was dissolved in 30 mL of EtOH and cooled with an ice–water bath. To the solution were added 0.83 g (21.9 mmol) of sodium borohydride in portions and then 3.00 g (19.9 mmol) of 1-bromopentane, both under a nitrogen atmosphere, and the solution was stirred at room temperature for 3 h. The reaction mixture was poured into water, extracted with ether, and the organic portion was washed successively with aqueous Na_2CO_3 and brine. The ether solution was dried over anhydrous Na_2SO_4 , the solvent was removed in vacuo, and the crude product was purified by a distillation using a 15 cm Vigreux column: Yield 3.53 g (78%), bp 56.5–57.5 °C (0.16 Torr) [lit.¹⁷ 116 °C (5.0 Torr)], faintly yellow oil; ¹H NMR δ 0.88 (t, 3H, $J = 7.0$ Hz), 1.35 (m, 4H), 1.71 (tt, 2H, $J = 7.5$, 6.7 Hz), 2.91 (t, 2H, $J = 7.5$ Hz), 7.15–7.33 (m, 3H), 7.42–7.53 (m, 2H); ¹³C NMR δ 13.9, 22.1, 27.8, 29.8, 32.0, 126.5, 128.9, 130.6, 132.3; IR (neat) 466, 474, 671, 691, 735, 779, 999, 1022, 1074, 1105, 1156, 1194, 1244, 1267, 1298, 1379, 1437, 1466, 1478, 1580, 1743, 1794, 1873, 1945, 2859, 2872, 2928, 2959, 3000, 3017, 3059, 3072 cm^{-1} ; MS, *m/e* (relative intensity) 27 (10), 29 (15), 39 (10), 41 (23), 43 (92), 51 (12), 71 (12), 55 (8), 71 (12), 77 (22), 78 (41), 91 (12), 154 (22), 155 (23), 156 (50), 157 (17), 158 (100), 159 (9), 160 (18), 224 (9, M⁺), 225 (8, M⁺), 226 (23, M⁺), 228 (46, M⁺), 230 (9, M⁺). Anal. Calcd for $\text{C}_{11}\text{H}_{16}\text{Se}$ (%): C, 58.15; H, 7.10. Found (%): C, 57.82; H, 7.01.

***tert*-Butyl Phenyl Selenide (**1c**).**^{19,20} A solution of 2.47 g (26.1 mmol) of phenylselenenyl chloride in 50 mL of dry ether cooled with an ice–water bath was added to 7.6 mL of *tert*-butyllithium (1.7 M, 31.3 mmol) in pentane, and the mixture was stirred at room temperature under a nitrogen atmosphere for 0.5 h. The reaction mixture was poured into water, extracted with ether, and the organic portion was washed successively with aqueous Na_2CO_3 and brine. The ether solution was dried over anhydrous Na_2SO_4 , and the solvent was removed in vacuo to give 4.52 g of crude product. The crude product was purified by a distillation using a 15 cm Vigreux column to give 2.78 g (31%) of pure **1c** as a faintly yellow oil: bp 33–34 °C (0.23 Torr) [lit.²⁰ 57–58 °C (0.8 Torr)]; ¹H NMR

(16) Analytical and spectroscopic data are provided as Supporting Information.

(17) Foster, D. G. *Recl. Trav. Chim. Pays-Bas*. **1935**, 447–457.

(18) Duddeck, H.; Wagner, P.; Rys, B. *Magn. Reson. Chem.* **1993**, 31, 736–742.

(19) Ranu, B. C.; Mandal, T.; Samanta, S. *Org. Lett.* **2003**, 5, 1439–1441.

(20) Gabdrakhmanov, F. G. *Sb. Aspir. Rab. Kazan. Gos. Univ. Khim. Geol.* **1967**, 85–90; *Chem. Abstr.* **1969**, 70, 96328g.

δ 1.41 (s, 9H), 7.23–7.43 (m, 3H), 7.65 (dd, 2H, $J = 7.8, 1.7$ Hz); ^{13}C NMR δ 32.1, 43.1, 128.3, 128.4, 128.6, 138.2; IR (neat) 476, 521, 673, 694, 741, 774, 914, 1001, 1022, 1065, 1075, 1154, 1219, 1302, 1364, 1391, 1437, 1452, 1460, 1476, 1580, 1758, 1808, 1881, 1952, 2859, 2890, 2917, 2936, 2957, 2973, 3058, 3073 cm^{-1} ; MS, m/e (relative intensity) 29 (20), 39 (12), 41 (37), 50 (5), 51 (11), 55 (5), 56 (7), 57 (100), 77 (22), 78 (44), 84 (6), 154 (19), 155 (19), 156 (42), 157 (14), 158 (84), 159 (8), 160 (15), 212 (7, M^+), 214 (15, M^+). High-resolution MS calcd for $\text{C}_{10}\text{H}_{14}\text{Se}$: 212.0267, 214.0260. Found: 212.0259, 214.0267.

Synthesis of Dialkyl Selenides 5a,b,d,e. Diallyl selenide (**5d**) was synthesized similar to that of dipentyl selenide (**5a**) and bis-(2-methylallyl) selenide (**5e**) by a conventional procedure.¹⁶

Dipentyl Selenide (5a).²¹ 1-Bromopentane (19.1 g, 126 mmol) was added to a suspension of 7.5 g (60 mmol) of Na_2Se in dry THF (100 mL). After completion of the addition, the reaction mixture was stirred at room temperature under a nitrogen atmosphere. The mixture was then poured into water, extracted with ether, and the organic portion was washed with brine and dried over anhydrous MgSO_4 . The solvent was then removed in vacuo, and crude product was purified by silica gel column chromatography (hexane): Yield 4.5 g (34%), faintly yellow oil; ^1H NMR (CDCl_3) δ 0.90 (t, 3H, $J = 7.2$ Hz), 1.33 (m, 4H), 1.66 (tt, 2H, $J = 7.5, 7.5$ Hz), 2.55 (t, 2H, $J = 7.5$ Hz); ^{13}C NMR (CDCl_3) δ 14.0, 22.2, 23.9, 30.4, 32.2; IR (neat) 564, 646, 727, 820, 903, 922, 962, 1034, 1059, 1072, 1105, 1190, 1240, 1267, 1294, 1333, 1342, 1377, 1420, 1464, 2624, 2664, 2731, 2857, 2870, 2924, 2955 cm^{-1} ; MS, m/e (relative intensity) 27 (10), 29 (15), 39 (6), 41 (34), 42 (10), 43 (100), 55 (12), 69 (29), 70 (31), 71 (81), 109 (7), 148 (8), 149 (12), 150 (15), 151 (16), 152 (26), 220 (7, M^+), 222 (15, M^+). Anal. Calcd for $\text{C}_{10}\text{H}_{22}\text{Se}$ (%): C, 54.29; H, 10.01. Found (%): C, 54.44; H, 10.20.

Photolysis. General Aspects. The following solvents for the photolyses were purchased and used as bought or after purification by standard procedures: *n*-hexane (spectral grade), *n*-heptane (spectral grade), cyclopentane (spectral grade), and cyclohexane (spectral grade), *n*-dodecane, *n*-tetradecane, *n*-hexadecane, cycloheptane, cyclooctane, and cyclodecane.

The following authentic samples were purchased and used as bought: benzene (spectral grade), *n*-pentane (spectral grade), 1-pentene, *n*-decane, 1-hexene, pentylbenzene, undecane, *cis*-2-pentene, *trans*-2-pentene, 3,4-diethylhexane, 2,2,3,3-tetramethylbutane, 1,5-hexadiene, 2,5-dimethyl-1,5-hexadiene, allylcyclohexane, diphenyl diselenide, di-*tert*-butyl selenide, and standard gases 2-methylpropane (0.997% in N_2) and 2-methylpropene (8.10% in N_2).

Excimer Laser Photolyses. Photolyses of **1** were conducted on 50 μL of 10^{-3} M solutions under a nitrogen atmosphere at room temperature using a synthetic quartz cell of 10 mm width and 1 mm optical path. The solutions were degassed with three freeze–pump–thaw cycles before photolysis. The lasers used were ArF, KrF, and XeCl excimer lasers [pulsewidth (fwhm): 20 ns (typical), 23 and 20 ns (typical), respectively]. Experiments on the fluence dependence were conducted similarly using a single laser pulse in the same experimental setup.

Analysis of the Photolysis Products. The consumption of **1** and the product yield were analyzed on a capillary GLC (Neutrabond-1, 60 m, 0.25 mmID, GL Sciences Inc.) and a HPLC pump (Supersphere 100, RP-8e, 250 mm, 4 mmID, Merck) fitted with a UV detector by comparison with authentic samples. MS analyses of the photoproducts of **1a-d**₁₁ were conducted using a GC–MS spectrometer equipped with a capillary column (Neutrabond-1, 60 m, 0.25 mmID, GL Sciences Inc.).

Supporting Information Available: Analytical and spectroscopic data of **1a-d**₁₁, **1b**, **1d**, **1e**, **5b**, **5d**, **5e**, and **8e**. Synthetic procedure of **5b**. Results on the low-pressure mercury lamp, and ArF and XeCl excimer laser photolyses of **1a** in *n*-hexane. Results on the KrF excimer laser photolysis of **1a** in *n*-hexane, *n*-heptane, *n*-dodecane, *n*-tetradecane, *n*-hexadecane, cyclopentane, cyclohexane, cycloheptane, cyclooctane, and cyclodecane. Results on the KrF excimer laser photolyses of **5a** and **7** in *n*-hexane. Results on the KrF excimer laser photolyses of **1a–e** in cyclohexane. NMR spectra of **1a–e**, **1a-d**₁₁, **5a,b,d,e**, and **8e**. This material is available free of charge via the Internet at <http://pubs.acs.org>.

JO701447A

(21) Gladysz, J. A.; Hornby, J. L.; Garbe, J. E. *J. Org. Chem.* **1978**, *43*, 1204–1208.